Quarterly Progress Report

For Period

September 30 to December 31, 1967

FUNDAMENTAL STUDIES OF THE METALLURGICAL, ELECTRICAL, AND OPTICAL PROPERTIES OF GALLIUM PHOSPHIDE

Grant No. NsG-555

Prepared For

NATIONAL AERONAUTICS AND SPACE ADMINISTRATION
LEWIS RESEARCH CENTER
CLEVELAND, OHIO

Work Performed By

Solid-State Electronics Laboratories
Stanford University
Stanford, California

PROJECT 5112: The Properties of Rectifying Junctions in $GaAs_xP_{1-x}$

National Aeronautics and Space Administration
Grant NsG-555
Project Leader: G. L. Pearson
Staff: S. F. Nygren

The purpose of this project is to study the preparation and characterization of rectifying junctions in GaP and $GaAs_xP_{1-x}$. In particular, we wish to relate the structure of the crystals to the electrical properties of the p-n junctions. During this quarter we have continued to improve our techniques for growing GaP layers by liquid epitaxy. We have quadrupled the thickness of such layers for a given temperature, and we have studied the spatial distribution of the zinc doping in the layers. We have extended our study of zinc diffusion into GaP by studying diffusion under high phosphorus pressure. A high pressure diffusion results in a shallower, but more planar, diffusion front than one produced at the same temperature and time but at low pressure.

A. Liquid Epitaxy

We have continued to develop the technology of growing liquid epitaxial layers of gallium phosphide. A programmable temperature controller has been connected to the liquid epitaxial furnace so that cooling rates during crystal growth may be precisely and reproducibly controlled.

We have found that cooling rate and seed position are important in controlling the thickness and quality of the grown layer. The results are analogous to those found with Stanford's GaAs liquid epitaxial system.[1] We shall limit ourselves here to listing in

Table 1 typical thicknesses of GaP layers that have been grown. Note that slow cooling and floating the seed result in a layer that is about four times as thick as a layer grown by quick cooling on a seed that is clipped to the bottom of the boat. Only slow cooling results in layers that are free of Ga inclusions.

Surface barrier capacitance measurements have been used to determine the doping levels at various depths in several samples. The results are shown in Fig. 1, and they suggest that zinc is not a very suitable dopant in our system. The vapor pressures over a typical growth solution at 1050°C are about $P_{Ga} \doteq 10^{-7}$ atm, $P_{P_2} = 4 \times 10^{-4}$ atm, $P_{Zn} = 5 \times 10^{-3}$ atm. The relatively high pressure of zinc means that it evaporates from the solution at a substantial rate, resulting in a visible deposit on the inside walls of the cold end of the reaction tube and in a sharp reduction of doping concentration as the crystal grows. We plan to try beryllium as an acceptor impurity in the future. Under conditions similar to those given above, it would have a vapor pressure of 5×10^{-10} atm and presumably would not evaporate from the solution.

B. Diffusion of Zinc into GaP

Below 1050°C, the Ga-P-Zn system as determined by Panish[2] has two monovariant phase regions as shown in Fig. 2. Diffusions of Zn into GaP are normally done in region 1, where the system contains liquid a, GaP, and Zn_3P_2 and has vapor pressures at 912°C (according to Ting[3]) of $P_{Zn} = 0.475$ atm and $P_{P_4} = 2.2 \times 10^{-6}$ atm. During this quarter we have done some diffusions at 912°C in region 2, where the system contains liquid b, GaP, and Zn_3P_2, and has $P_{Zn} = 0.260$ atm and $P_{P_4} = 2.2$ atm.

Diffusion at 912°C in region 1 typically results in moderately damaged sample surfaces. Etching a cross section of a diffused sample reveals two diffusion fronts, both of which are irregular. However, in relatively perfect regions of the sample, a unique diffusion depth for the deeper diffusion front can be defined: 53μ in one hour. Diffusion in region 2 results in a relatively undamaged sample surface. Here, however, the shallow diffusion front is planar, and the deeper one is less irregular than the deep front in region 1 diffusions. Again, unique diffusion depths can be defined, and it is found that depth varies as the square root of time as shown in Fig. 3. In one hour at 912°C, $X_{j1} = 12.4\mu$ and $X_{j2} = 15.4\mu$.

Present experimental data are insufficient to allow a quantitative analysis of the difference in diffusion depth between region 1 and region 2 although a qualitative estimate can be made. Chang[4] has shown that as long as the diffusion obeys Fick's Laws, p-n junction depth can be given by

$$X_j = A\sqrt{D_o t} \tag{1}$$

since the diffusion is steep fronted. Here D_o is the diffusion coefficient at the surface. It may then be shown by mass-action arguments that

$$X_j = A\sqrt{K_8 t D_i}\; P_{Zn}^{(n+1)/4}\, P_{P_4}^{(n-1)/16}\, \gamma_p^{(n+1)/4} \left[(n+1) + \frac{nC_s}{\gamma_p}\frac{\partial \gamma_p}{\partial C_s}\right]^{1/2} \tag{2}$$

where K_8 is an equilibrium constant, D_i is diffusion coefficient for interstitial zinc at the surface, P_{Zn} is the vapor pressure of Zn, P_{P_4}

is the vapor pressure of P_4, γ_p is the activity coefficient for holes at the surface, C_s is the concentration of substitutional zinc at the surface, and $+n$ is the charge state of interstitial zinc. The quantity n is disputed in the literature and may be taken as either 1 or 2. Either way, Eq. (2) cannot be fitted to the experimental data unless γ_p is taken to decrease as C_s increases. Panish and Casey[5] point out that this is expected, but no quantitative information is available.

It must be pointed out that Eq. (2) is not the only possible explanation for the experimental data. In fact, we can have little confidence in Eq. (2) until Eq. (1) is suitably verified. The data in Fig. 3 suggest that Eq. (1) is correct in that case. However, it is found that p-n junction depths for 805°C diffusions in region 1 are dependent upon the times for which the samples were pre-annealed as indicated in Fig. 4. This suggests that equilibrium is reached very slowly and casts some doubt on Eq. (1), at least for these conditions. More work will have to be done in order to clarify this problem.

REFERENCES

1. D. M. Chang, private communication.

2. M. B. Panish, J. Electrochem. Soc., 113, 224 (1966).

3. C. H. Ting, SEL Quarterly Status Report No. 104, Oct. 1 through Dec. 31, 1966, Contract Nonr-225(83), p. 21.

4. L. L. Chang, Solid State Electronics, 7, 853 (1964).

5. M. B. Panish and H. C. Casey, Jr., J. Phys. Chem. Solids, 28, 1673 (1967).

TABLE 1

Layer	Temperature	Initial Cooling Rate	Seed Area	Seed Position	Thickness	Inclusions	PN Junction	Solution Ga	Solution GaP	Solution Zn
LEP5	1054°C	12°/min	about 15mm^2	Sunk	45μ	Yes	No	5.06g	0.346g	4.02mg
LEP6	1054°C	12°/min	about 15mm^2	Sunk	65μ	Yes	No	Reused solution from LEP5		
LEP8	1057°C	2°/min	about 15mm^2	Sunk	115μ	No	110μ	5.06g	0.350g	3.85mg
LEP12	954°C	0.75°/min	15.3mm^2	Sunk	58μ	No	No	4.95g	0.129g	2.87mg
LEN1	948°C	5°/min for 2 min then 0.75°/min	23.3mm^2	Float	92μ	Yes	No	5.05g	0.141g	0

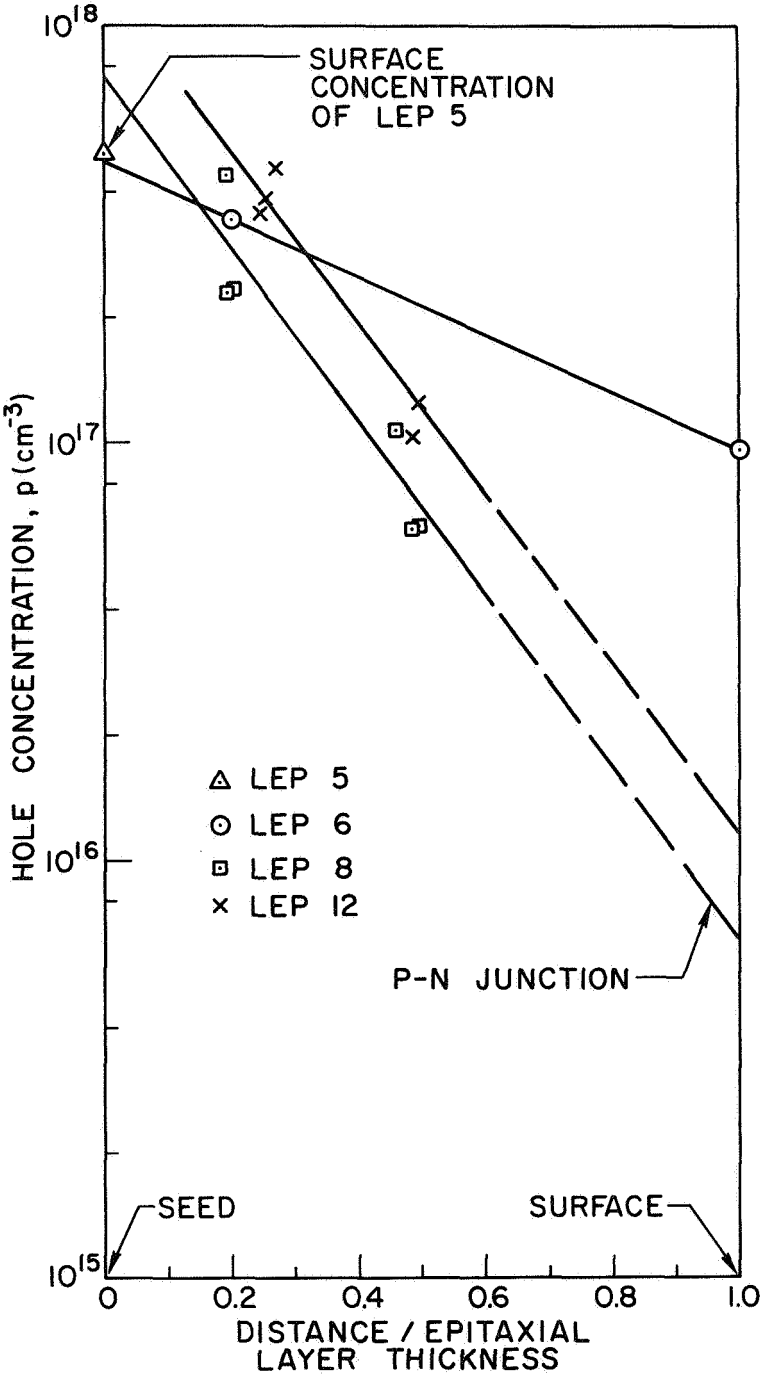

FIG. 1 - Hole concentration vs. fraction of epitaxial layer grown.

B43237

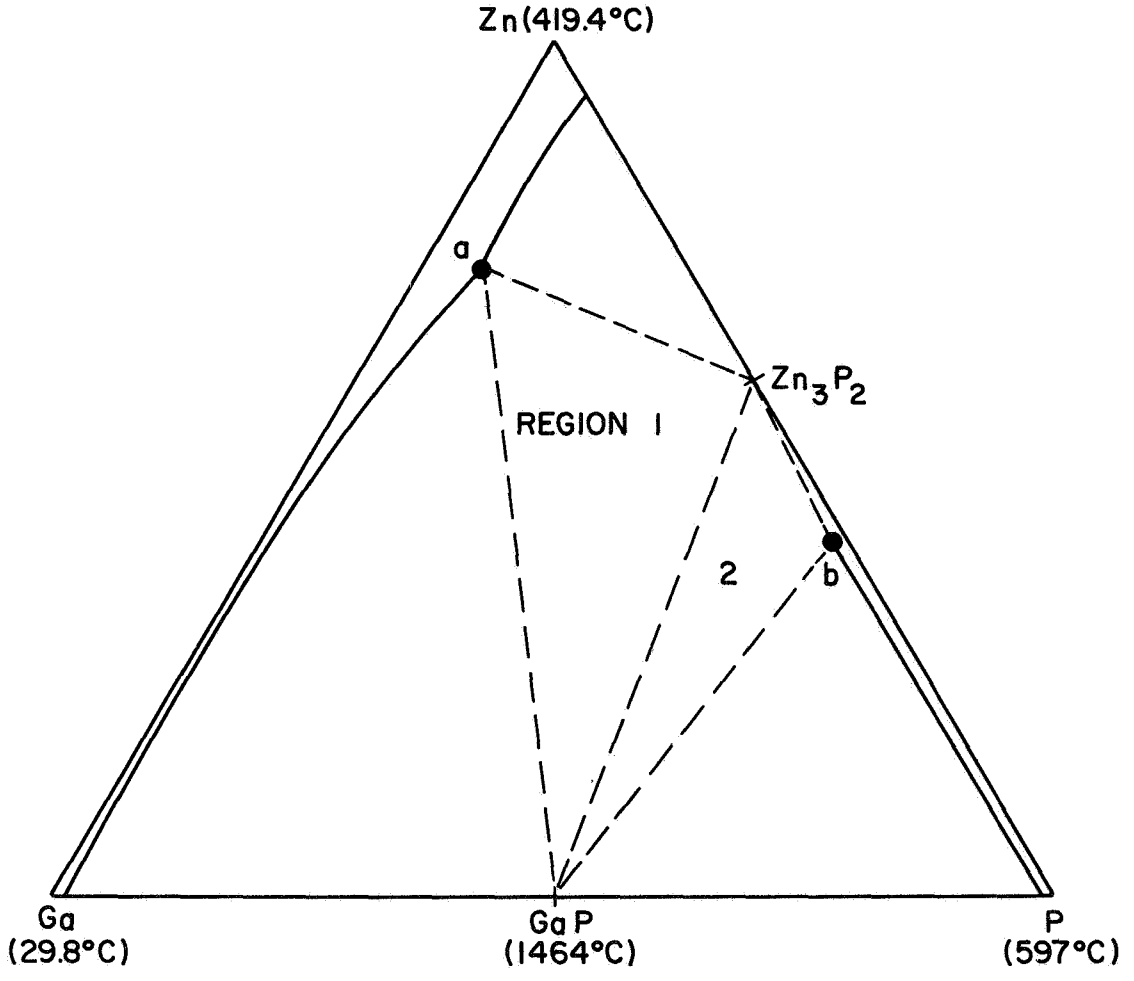

FIG. 2 - The Ga-P-Zn phase diagram at 912°C (after Panish).

A43232

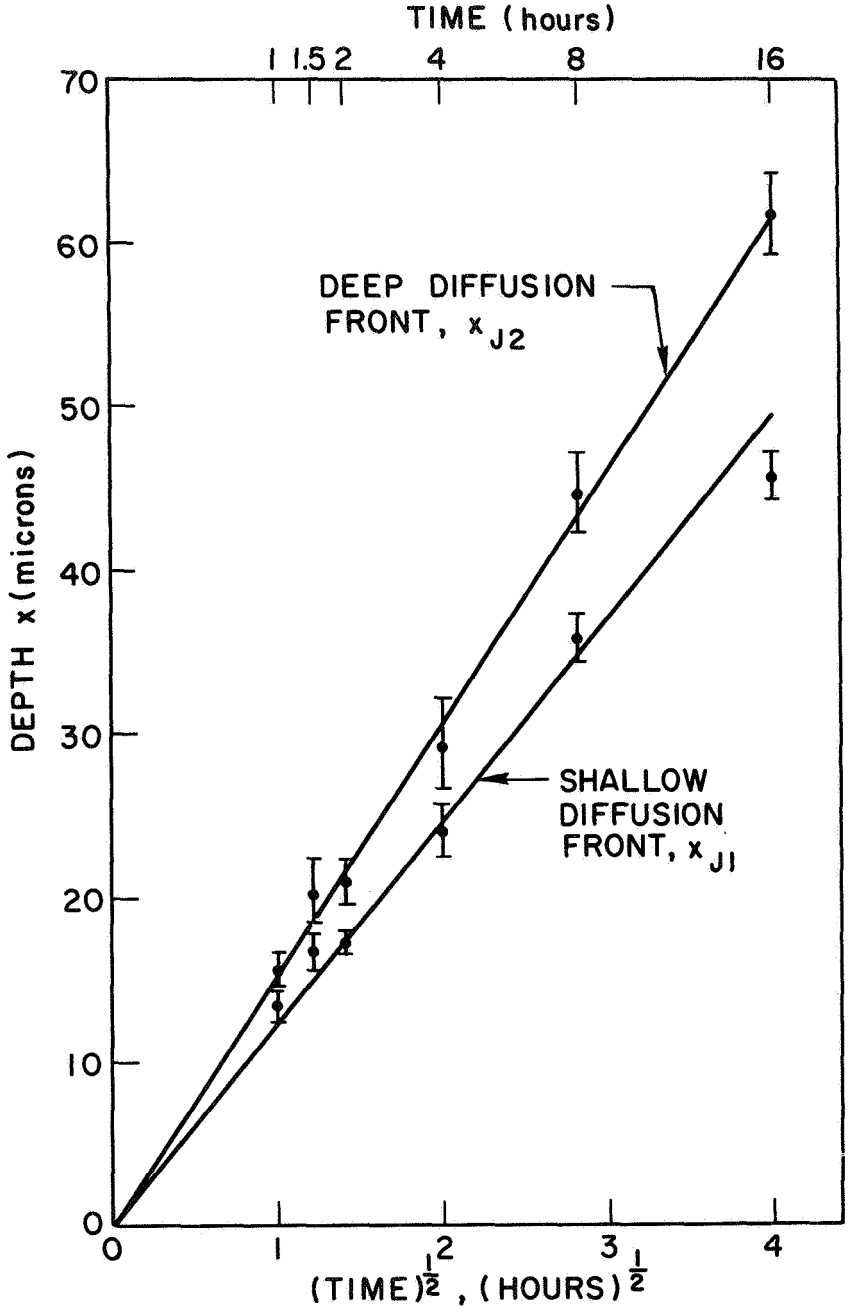

FIG. 3 - Shallow diffusion depth and deep diffusion depth vs. square root of time. Zine diffusion into GaP at 912°C in region 2 of phase diagram.

A43233

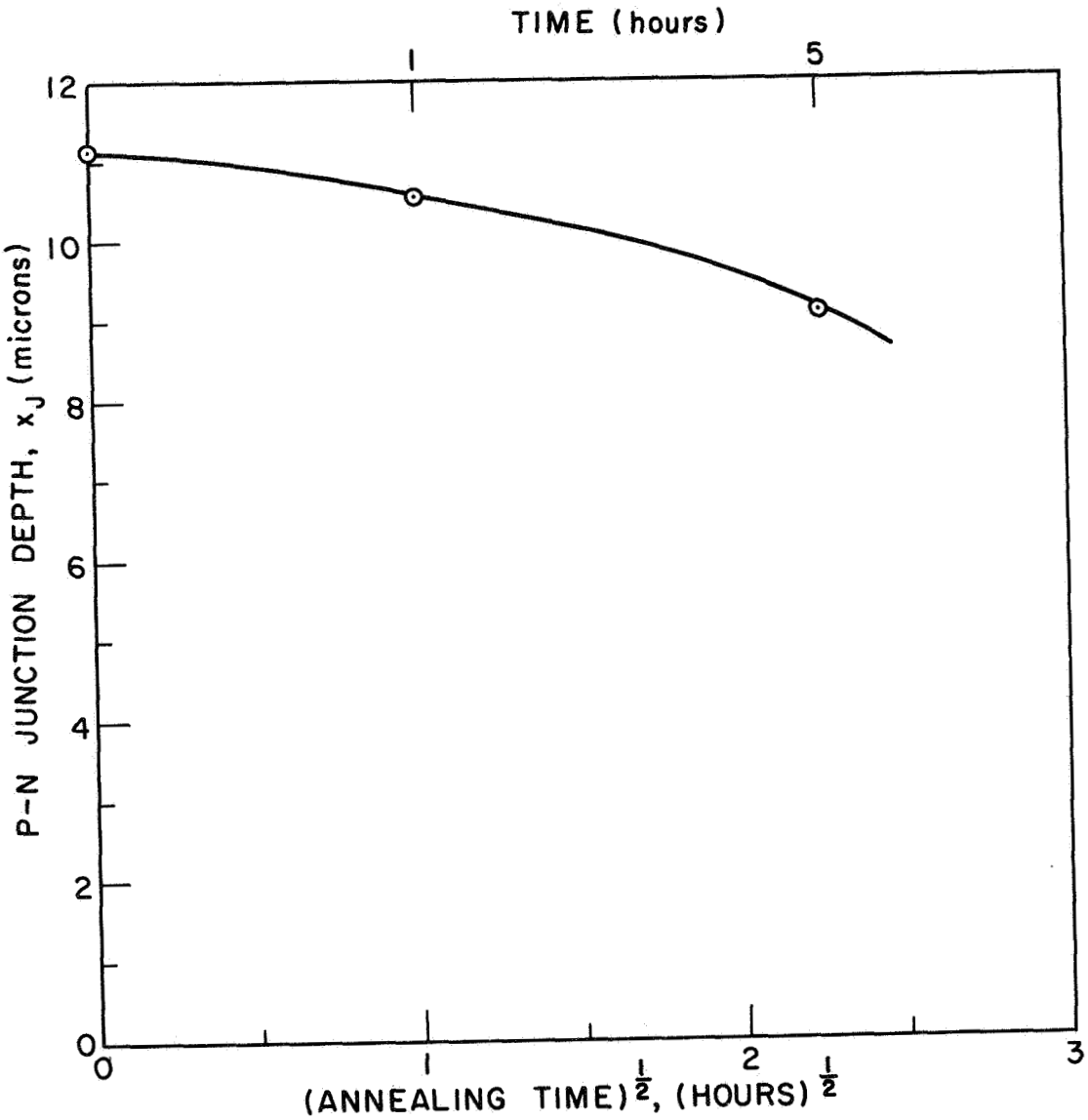

FIG. 4 - P-N junction depth vs. square root of pre-annealing time. Samples were pre-annealed at 805°C for the time given. Then they were quenched, loaded into ampoules for zinc diffusion in region 1 of the phase diagram, and diffused for 2.75 hours.

A43234

PROJECT 5115: SEMICONDUCTOR DEVICES FOR HIGH TEMPERATURE USE

National Aeronautics and Space Administration
Grant NsG-555
Project Leader: G. L. Pearson
Staff: Y. Nannichi

The purpose of this project is to prepare power rectifiers and solar batteries which will operate at temperatures up to 500°C.

A. Crystals

A set up for growing n-type GaP by liquid epitaxy has been completed. One undoped crystal was grown.

Also, a set up for growing both n- and p-type crystals of GaAs, GaP and their alloys by vapor epitaxy has been completed. This set up will also be used to grow undoped crystals for use as substrates in the liquid epitaxy system. After several unsuccessful attempts with the vapor epitaxial system, one undoped GaP crystal was grown. Cd doped crystals will be grown in the future.

During the early part of this quarter, undoped GaP crystals grown by vapor epitaxy were kindly supplied by C. H. Ting and S. F. Nygren who are working under other projects. Most of the experiments performed during this quarter were done with these crystals.

B. Capacitance Measurements

Many Schottky diodes were made in order to determine the impurity concentrations of the crystals. Ohmic contacts were made alloying Ni-Au-Ge on GaP at 450°C, and the Schottky barriers were formed on a plane by evaporating Au through a mask in the vacuum better than 10^{-8} mmHg.

The impurity concentrations of the crystals were determined by using the following equation:

$$N_d = \frac{2}{q\kappa\epsilon_o}\left(\frac{C}{V}\right)^2(\Phi - V), \quad (\kappa = 10 \text{ and } \Phi = 1.4 \text{ volts})$$

Table 1 shows the impurity concentration of the crystals.

A remarkable difference exists between crystals grown by liquid and vapor epitaxy. The capacitance of Schottky barriers on vapor epitaxial crystals always drifts with time after change in light intensity. As an example (see Fig. 1), ambient light is enough to cause the capacitance of one barrier to change by 10%, suggesting the existence of deep levels whose concentration may be as high as 20% of the majority carrier density.[1] In contrast, drift was not observed in the capacitance of barriers placed on the liquid epitaxial crystal. This is consistent with the results of J. Harris on GaAs.[2]

C. Breakdown Voltage

The breakdown voltage of each Schottky barrier diode was measured, and the correlation between the breakdown voltage and the impurity concentration of the crystal was sought.

Figure 2 shows plots of breakdown voltage vs. impurity concentration. Solid lines link values from the same crystals. The broken lines show the theoretical relation between breakdown voltage and impurity concentration for a step junction as calculated by S. Size,[4] taking junction curvature r_J as a parameter.

It is evident that the crystal quality rather than the impurity concentration primarily determines the breakdown voltage at this stage. We cannot determine yet which is the most important factor, deep level impurities, crystalline disorders, or inhomogeneous distribution of impurities.

D. High Temperature Operation of Schottky Diodes

A preliminary survey was made to determine which metals would be useable as Schottky electrodes for high temperature devices. We chose nickel first; it is less difficult to evaporate in vacuum than other metals such as W, Mo and Ta, and it does not alloy with GaP until temperatures above 550°C. For the ohmic contact to n-type GaP, Ni-Ge alloy was evaporated onto the crystal and then alloyed at 750°C for 4 minutes in H_2. Pure nickel was applied to the A face of the crystal as the Schottky electrode. The barrier height of 1.4 eV which was observed with the gold electrode did not change appreciably with the nickel electrode.

Figure 3 shows the V-I characteristics of GaP Schottky diode at various elevated temperatures in forming gas. These results indicate that high temperature operation is feasible.

E. Plans for the Next Quarter

More crystals will be grown by both liquid and vapor epitaxy. Hetero GaAs - GaP pn junctions will be grown by vapor epitaxy after control of impurity doping is attained. Impurity doping will be tried by adding cadmium iodide and sulfur trichloride to the bubbler of PCl_3 or $AsCl_3$.

The factors which determine the breakdown voltages of Schottky diodes will be investigated. It is rather difficult to define the junction curvature, r_j, in a Schottky barrier diode which utilizes an inversion region at the surface whose thickness is on the order of several tenths of microns. Since a guard ring structure should reduce the concentration of the electric field, we shall attempt to make a doughnut type guard ring structure by using photolithography.

REFERENCES

1. F. Padovani, private communication.
   A. Goodman, Journal of Applied Physics, 34, 329 (1963).

2. J. Harris, Quarterly Progress Report, July-September 1967, Project K702, Stanford University.

3. S. Sze, Appl. Phys. Letters, 8, 111 (1966).
   S. Sze and G. Gibbons, Solid State Electronics, 9, 831 (1966).

TABLE 1 Impurity Concentration of the Crystals

Crystal Number	N_D cm^{-3}
SN-13	1.7×10^{15}
CT-1	3×10^{15}
CT-3	8×10^{14}
CT-4	2×10^{15}
CT-5	1.2×10^{15}
CT-6	2.3×10^{15}
CT-7	$0.5 \sim 1.2 \times 10^{16}$
CT-10	6×10^{14}
CT-11	1.4×10^{15}
CT-12	2×10^{15}
CT-13	2.2×10^{15}
LG-1	3.8×10^{16}

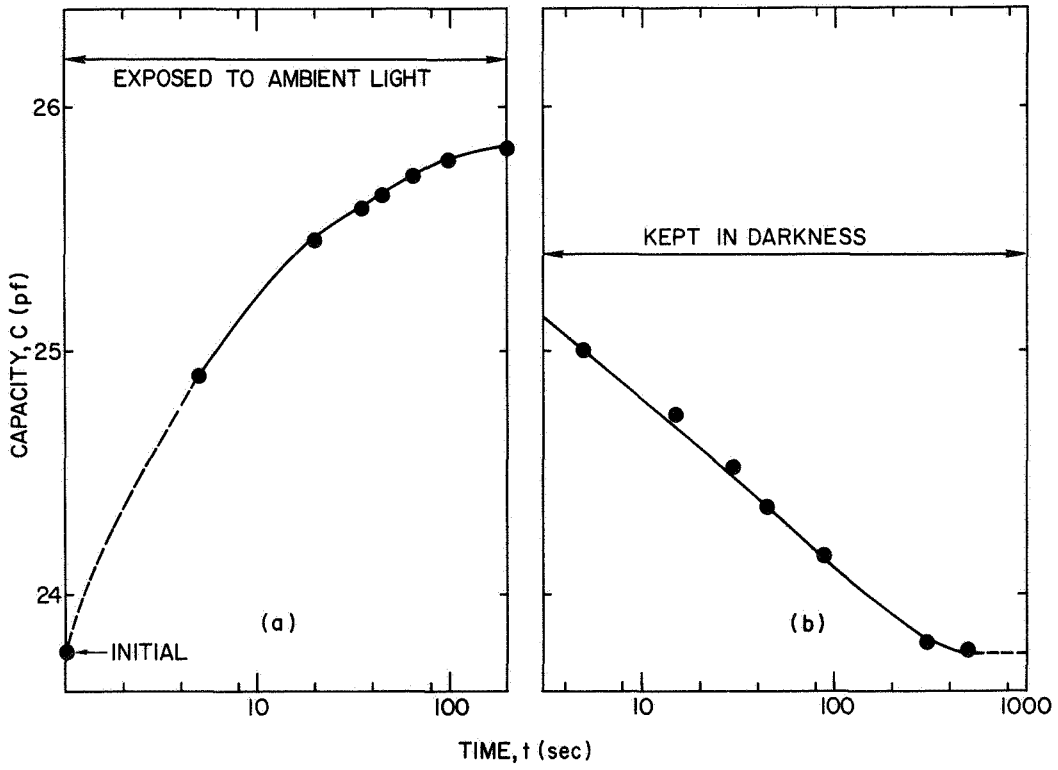

FIG. 1 - Drift in Schottky Barrier Capacitance with Time.
a) ambient light
b) in the dark

B43246

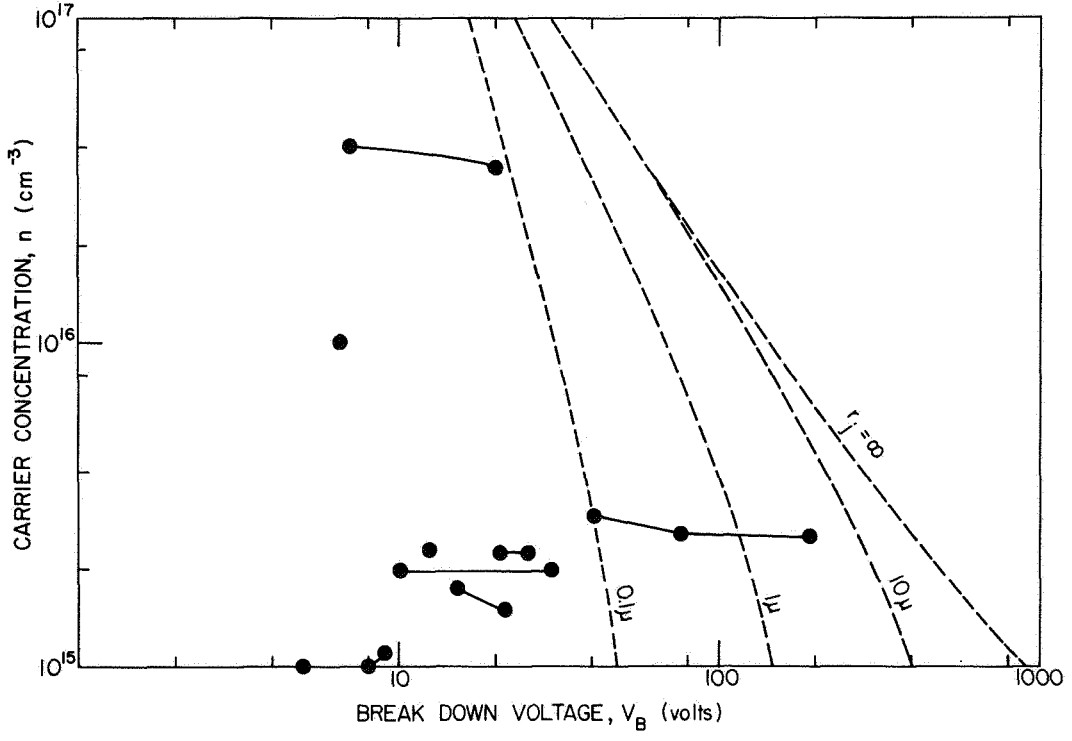

FIG. 2 - Reverse Breakdown Voltage vs. Carrier Concentration for Schottky Barriers on Sulfur Doped GaP.

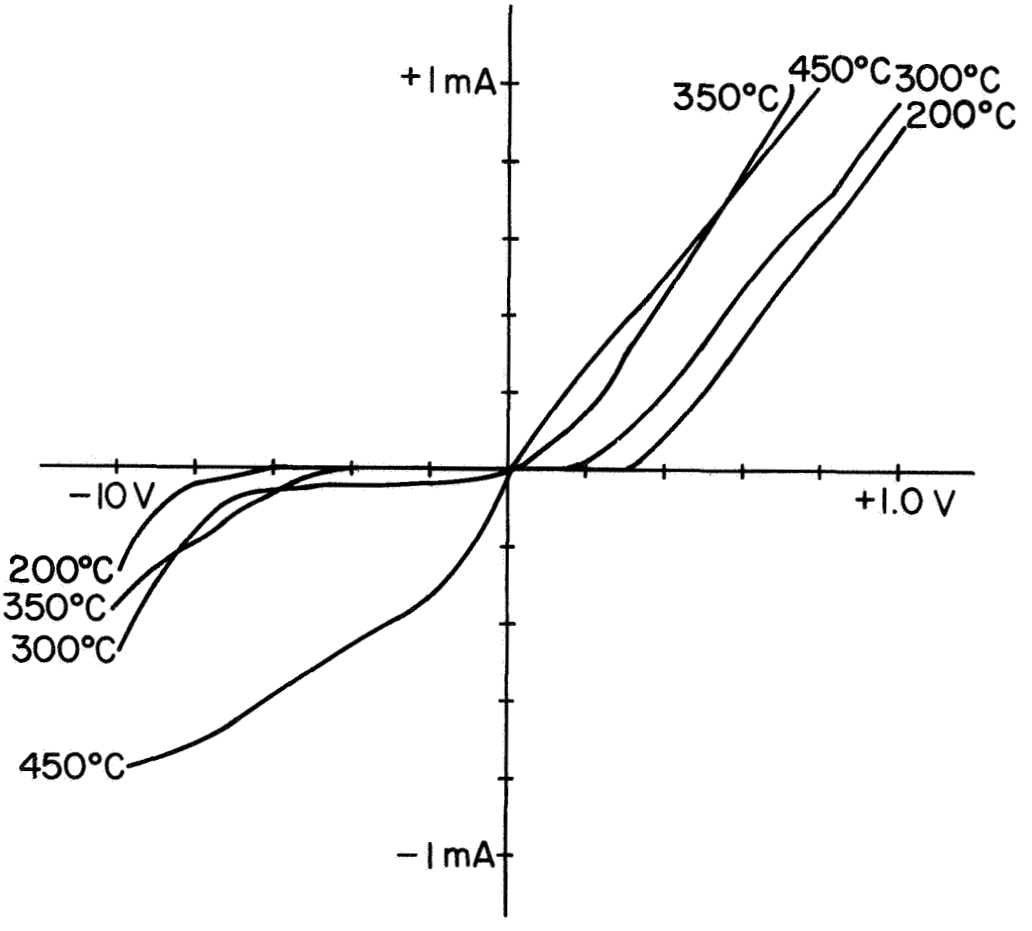

FIG. 3 - Current vs. Voltage Characteristics of GaP Schottky Barrier Diodes at Elevated Temperatures.

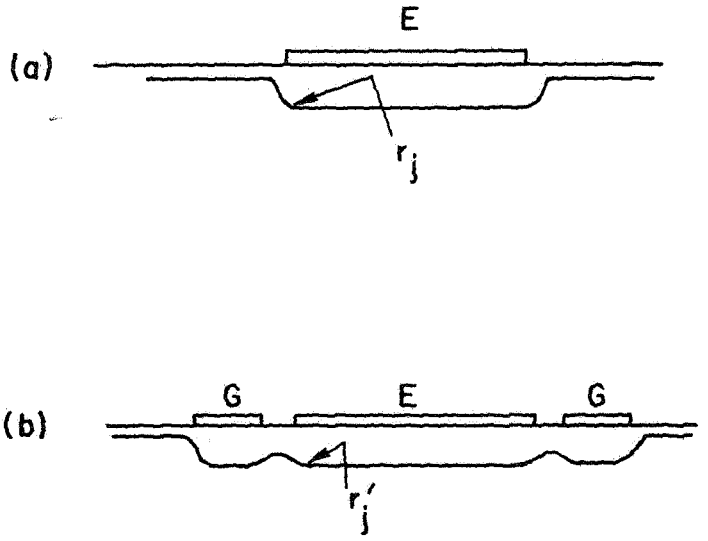

FIG. 4 - Junction Contours
a) without guardring
b) with guardring

A43249

PROJECT 5116: DONOR IMPURITIES IN GaP

National Aeronautics and Space Administration
Grant NsG-555
Principal Investigator: G. L. Pearson
Staff: A. Young*

The purpose of this project is to study the behavior of shallow donors in gallium phosphide. In particular, S, Se, and Te will be diffused into GaP to determine solubility and diffusion parameters. This information will be useful in delineating the properties of GaP doped with these shallow donor impurities.

Incremental Hall Measurements on Diffused Layer

The electron concentration and mobility as a function of depth in a GaP sample doped with sulfur by diffusion at 1200°C have been determined using an incremental Hall measurement technique developed by M. Buehler[1] of these laboratories. The results along with the radiotracer profile obtained on the same sample are shown in Fig. 1.

The results of carrier concentration and electron mobility may be somewhat in error because the four contacts were not exactly centered on the sample. The region near the surface may also be affected by surface irregularities developed during the diffusion. However, the results do illustrate that the sulfur is doping the sample; the sheet resistivity is much lower after the diffusion. Also, as the diffused layer is etched away in increments during the measurement, the sheet resistivity increases and a very sharp increase is observed near the penetration depth as determined from the radiotracer profile.

The low doping efficiency of a sulfur-diffused layer in GaP should be noted. Less than 10% of the total sulfur atoms are electrically

*NSF Fellow

active. Even less than this is observed in samples grown from Ga-rich solutions at 1040°C.[2]

Compensation by copper or other deep lying impurities is not believed to be a major influence. However, in the future, diffusions for electrical measurements will be done in Spectrosil ampoules.

Diffusions

During the previous quarter a number of diffusions of S-35 in GaP were performed at 1215°C to study:

1) The difference between diffusion into a mechanically polished and a chemically polished surface.

2) The effect of pre-annealing prior to diffusion in a phosphorus atmosphere identical to that used during diffusion but in the absence of sulfur.

3) The time variation of sulfur diffusions in GaP.

4) The variation of the diffusion profiles with sulfur pressure during diffusion.

5) The variation of the diffusion profile with phosphorus pressure during diffusion.

In a previous quarterly report, the variation of diffusion profiles with temperature, and with sulfur and phosphorus pressures at a fixed temperature (T = 111°C) were reported. The results were profiles obtained by the mechanical lapping technique. The current results have been obtained by a chemical etching technique which permits determination of much shallower profiles. In general, better data has been obtained this quarter, but results are in agreement with previous work.

Effect of Surface Treatment Before Diffusion (D-23 and D-24)

D-23 was mechanically polished with Linde A and then chemically polished so that approximately 8 microns was removed from the surface. D-24 was simply mechanically polished. Diffusions were carried out in separate ampoules but under the same conditions. The results given in Fig. 2 show that the profiles are identical within experimental error.

Effect of Preannealing (D-18 and D-20, D-16 and D-17)

D-18 was not preannealed, D-20 was preannealed under diffusion conditions for 24 hours and then repolished before diffusion. The samples were then diffused separately but under identical conditions. The results shown in Fig. 2 are again identical within experimental error.

D-16 was not preannealed, D-17 preannealed under diffusion conditions for 24 hours and then repolished before diffusion. Results shown in Fig. 2 are again the same.

The necessity of repolishing the samples between the preanneal and the final diffusion unfortunately complicates the interpretation of results. However, there is reason to believe that equilibrium of the GaP crystal with the vapor is rapid compared to the diffusion of sulfur into the crystal; diffusion of zinc into GaP (not annealed) is affected significantly by a phosphorus overpressure. This implies that the rate of vacancy equilibrium is comparable to that of the zinc in diffusion. Since zinc diffuses more rapidly than sulfur, vacancy equilibrium should be more rapid than the sulfur in diffusion.

Time Variation

A number of diffusions were performed under identical conditions but for different times to study the time variation of the diffusion profiles. Two such sets of data are shown in Figs. 2 and 3. The results indicate that the profiles are a function of $\lambda = (x/\sqrt{t})$; that is, they obey Fick's Law.

Effect of Sulfur Pressure

Diffusion profiles in Fig. 4 illustrate the effect of changing the sulfur pressure during diffusion while keeping all other variables fixed. As was noted in a previous report, the surface concentration is proportional to the sulfur vapor density or pressure (P_{s_2}), which is in disagreement with a simple model incorporating sulfur atoms on phosphorus sites. Also the previously noted (at 111°C) variation of profile shape with sulfur pressure is again seen at this higher temperature, indicating a concentration dependent diffusion coefficient.

Effect of Phosphorus Pressure

Two sets of profiles illustrating the effect of phosphorus pressures are shown in Figs. 5 and 6. These are very similar to data relating to sulfur and selenium in GaAs.[3,4] The penetration depth is relatively independent of pressure. If a dependence on pressure is present it is too small and in the opposite direction to that expected for a simple vacancy-type diffusion where sulfur atoms migrate on the phosphorus sublattice. (The simple theory predicts $D \alpha V_p \alpha (P_{p_2})^{-1/2}$, since in our own experiment P_{p_2} varies from 0.02 - 1.2 ATM. We should see a variation of $\sqrt{60}$ in D or a variation of 2.8 in penetation depth well within experimental resolution.)

REFERENCES

1. M. G. Buehler, SEL TEchnical Report No. 5101-1 (SU-SEL-66-064), Stanford, California, July 1966.

2. F. A. Trumbore, et al, J. Electrochem Soc., 112, 782 (1965).

3. L. J. Vieland, J. Phys. Chem. Solids, 21, 318 (1961).

4. R. W. Fane and A. J. Goss, Solid State Electronics, 6, 383 (1963).

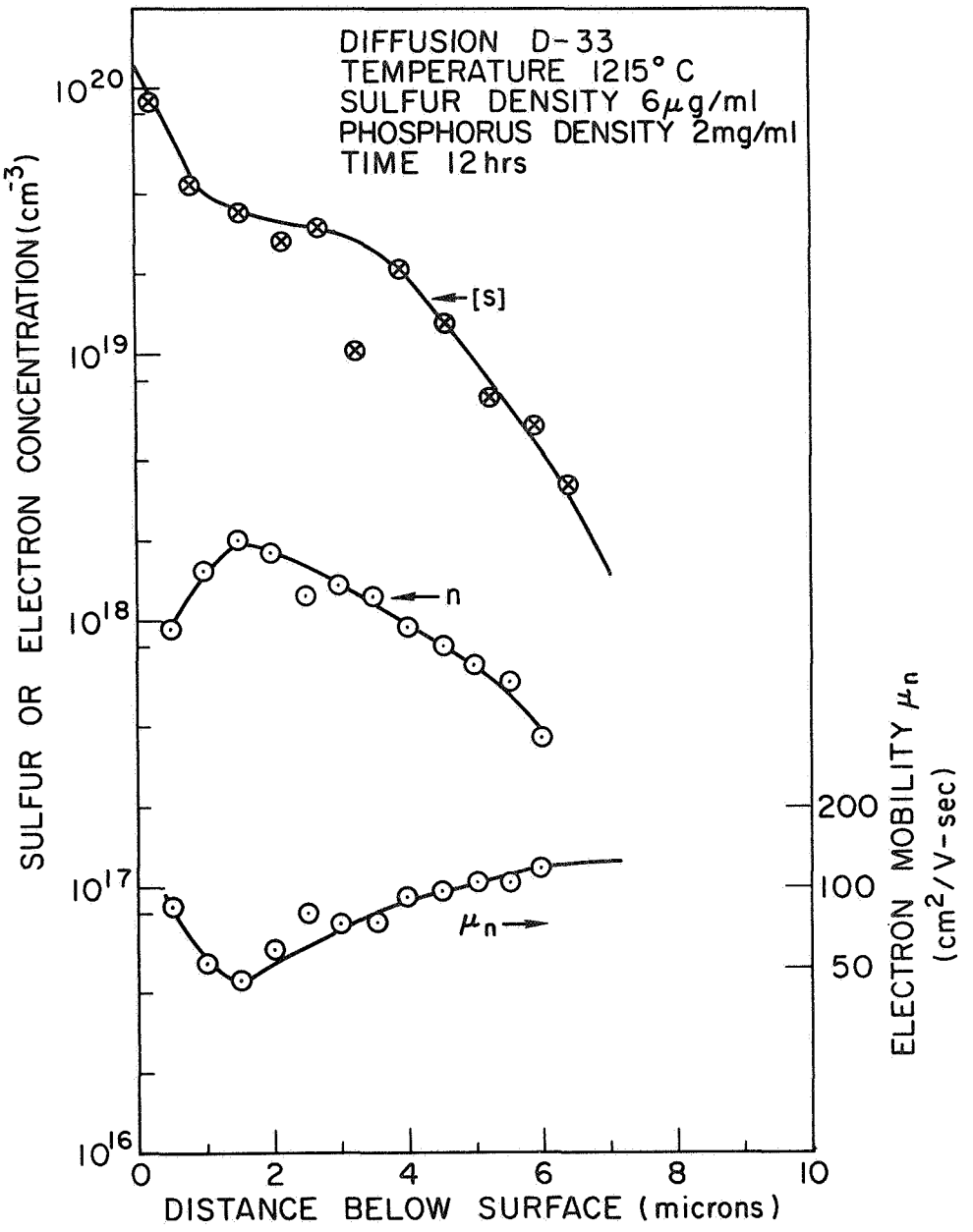

FIG. 1 - Total Sulfur Concentration, Electron Concentration and Mobility in Diffused Layer.

B43241

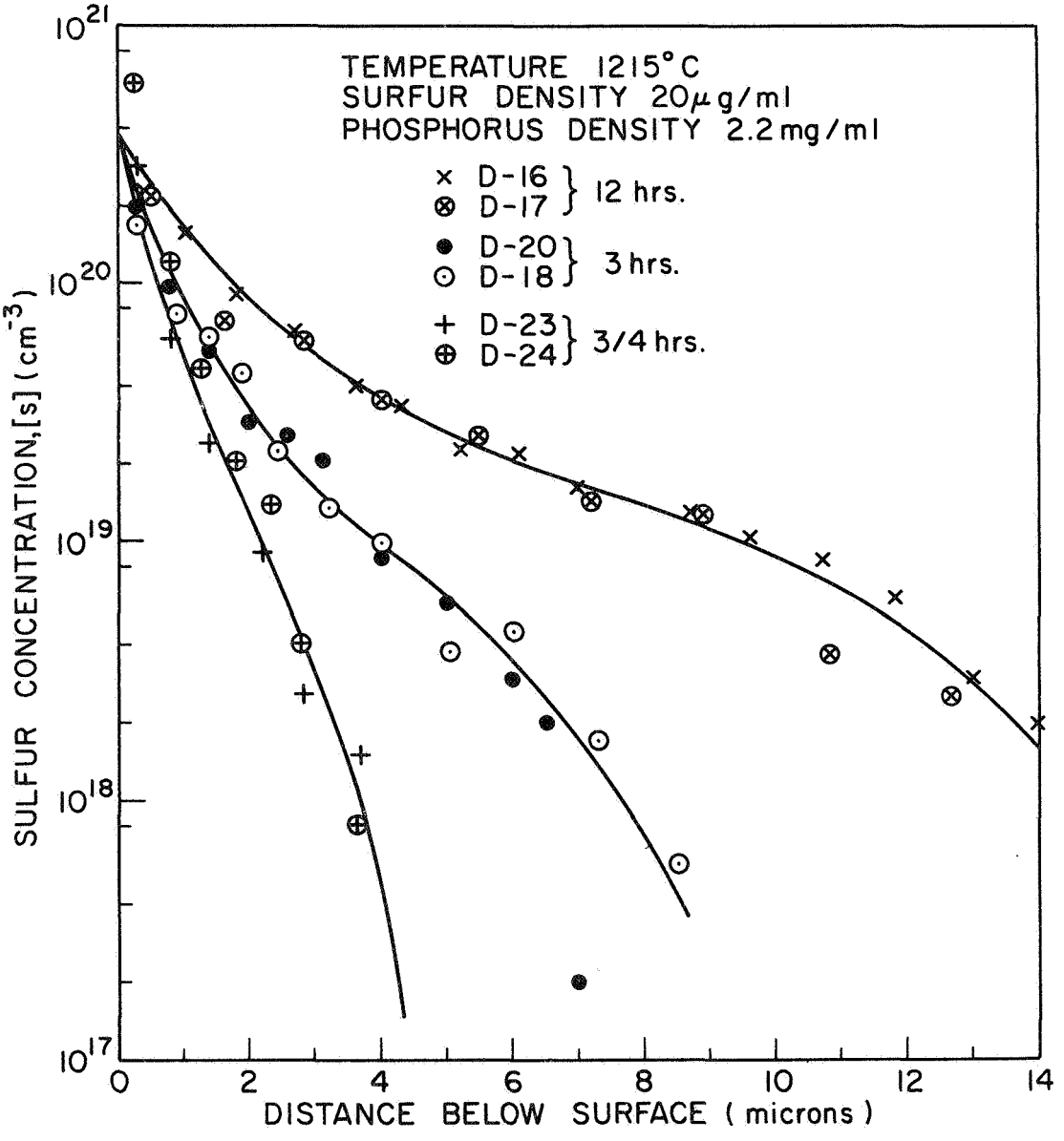

FIG. 2 - Time Variation of Diffusion Profiles (Sulfur in GaP).

B43248

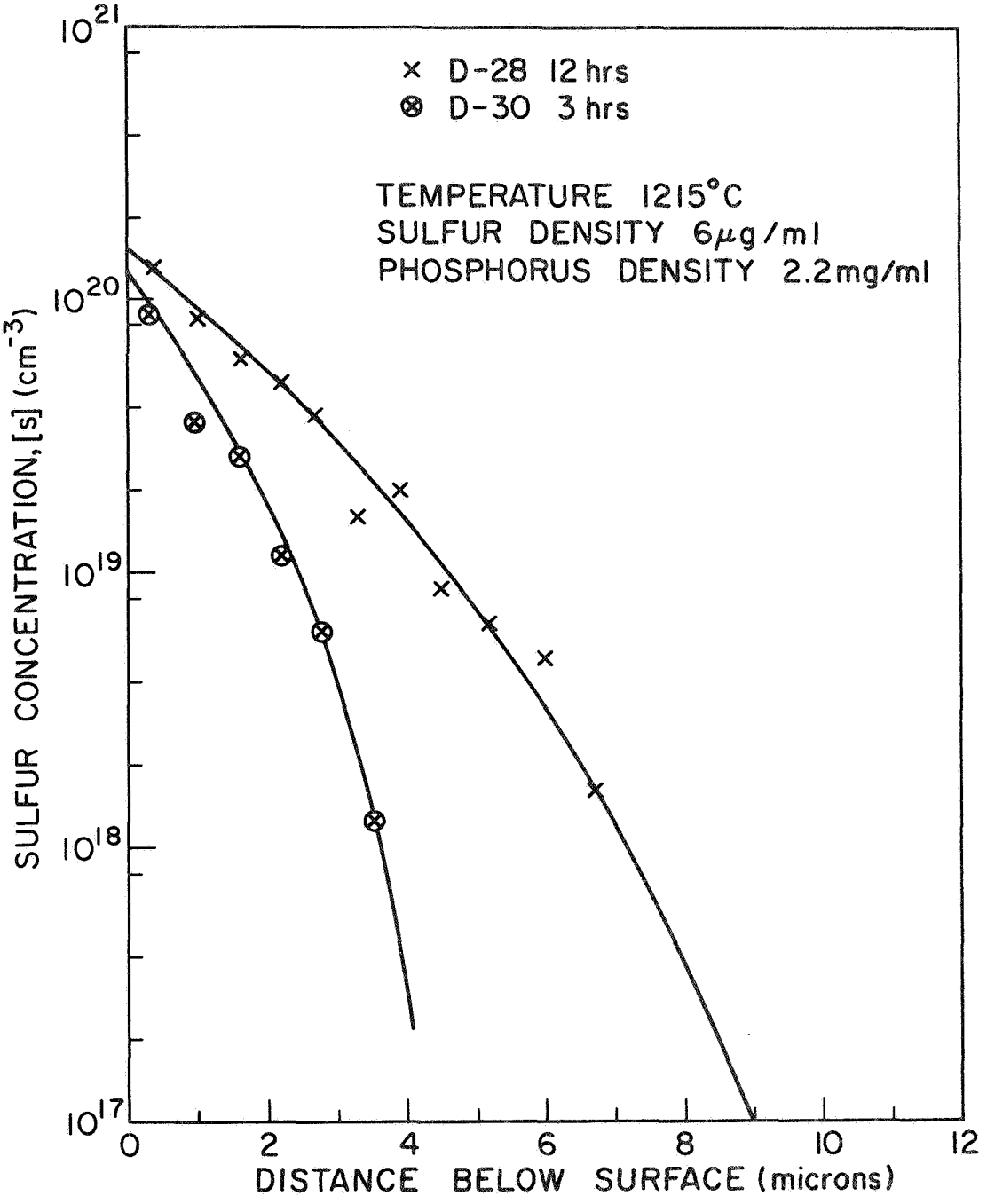

FIG. 3 - Time Variation of Diffusion Profiles (Sulfur in GaP).

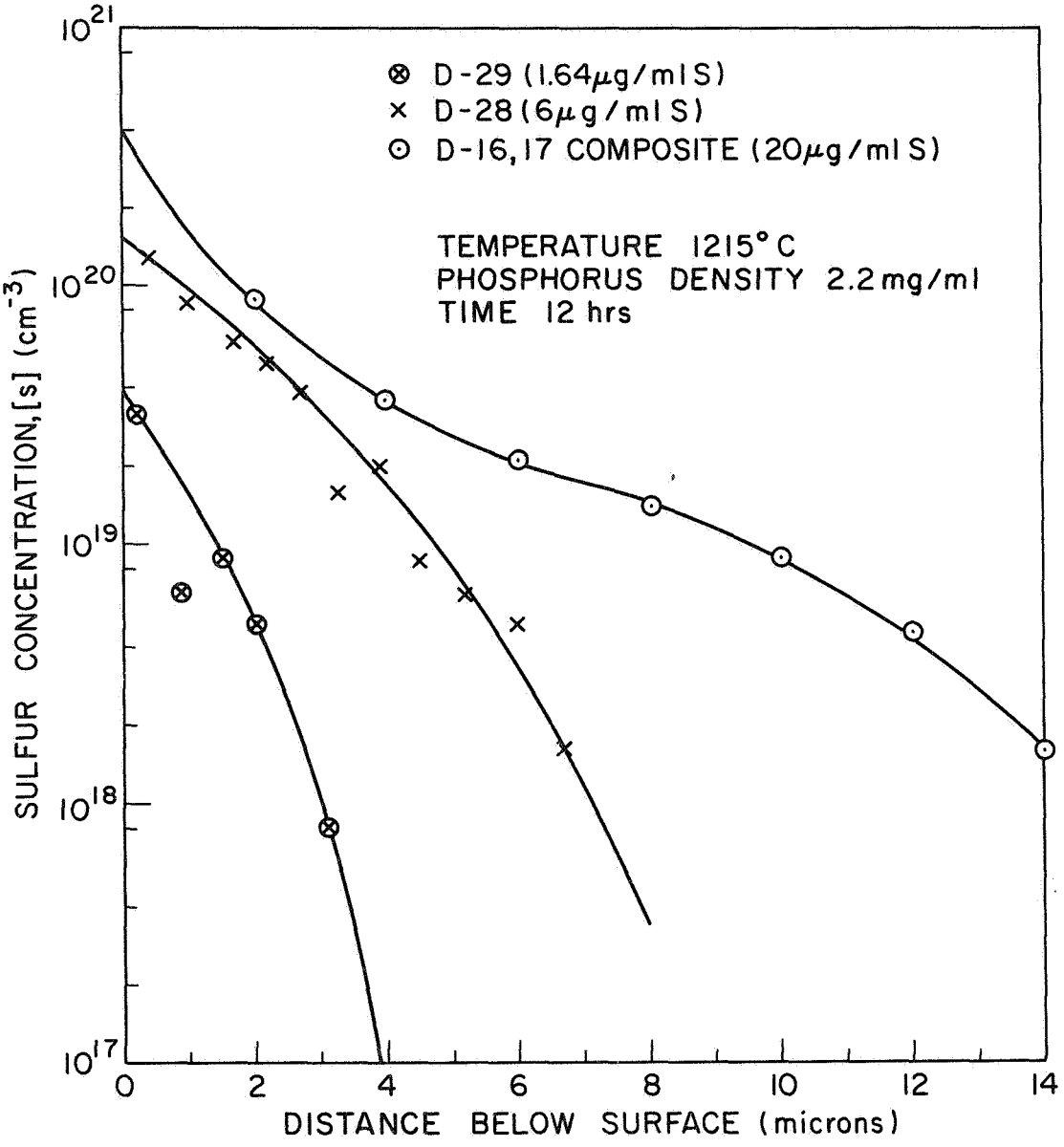

FIG. 4 - Variation of Diffusion Profiles with Sulfur Pressure (Sulfur in GaP).

B43242

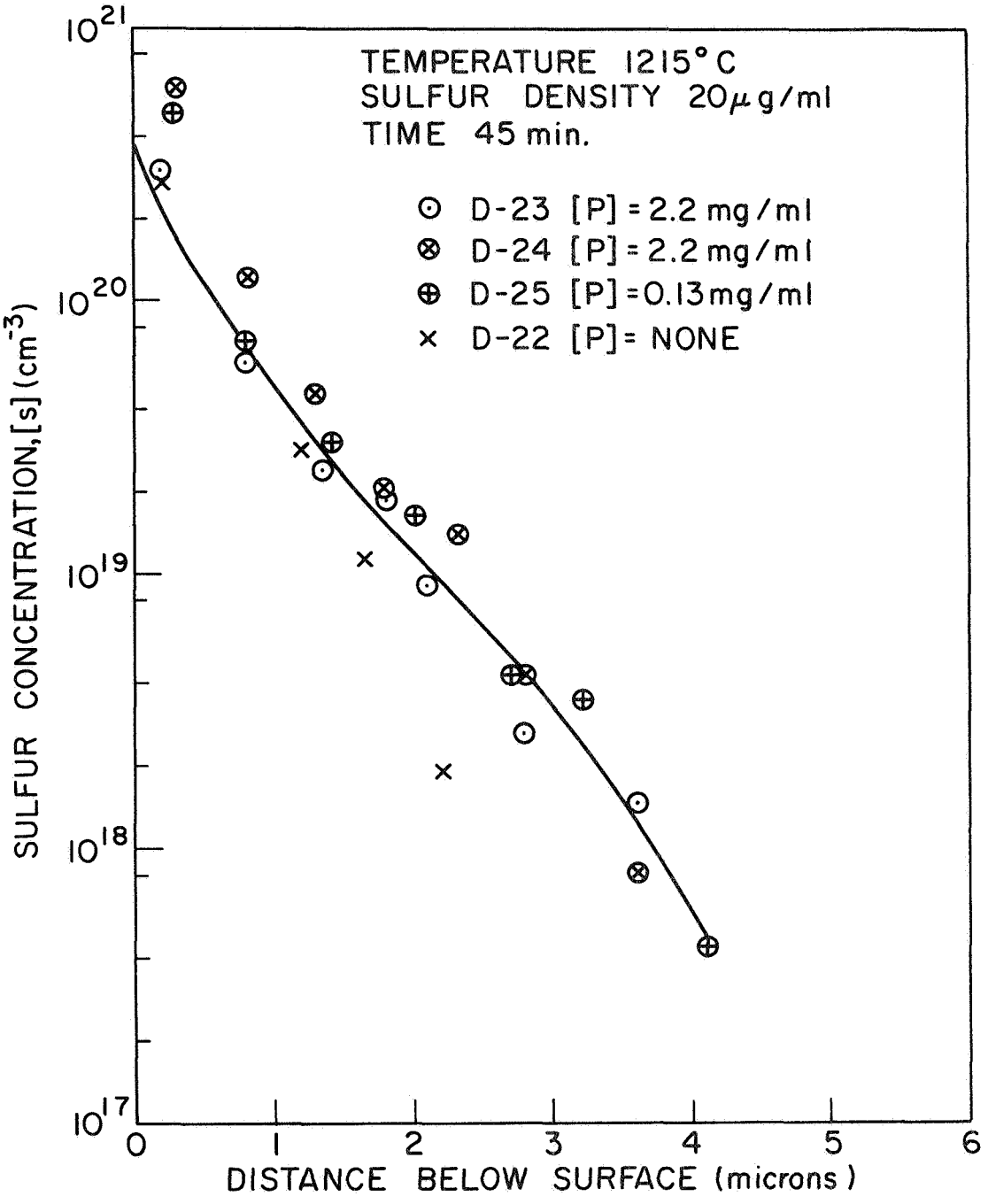

FIG. 5 - Variation of Diffusion Profiles with Phosphorus Pressure (Sulfur in GaP).

B49L43

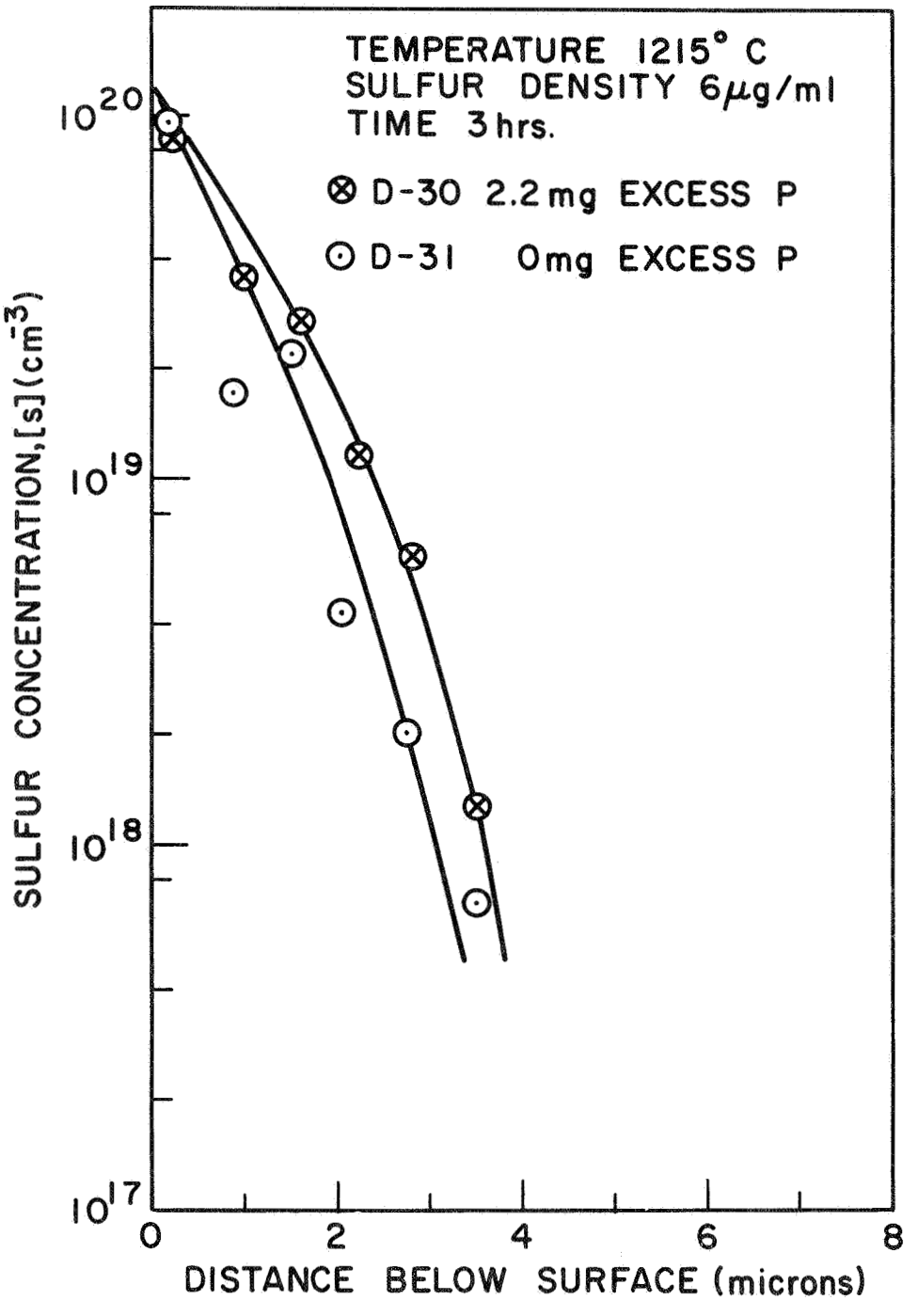

FIG. 6 - Variation of Diffusion Profiles with Phosphorus Pressure (Sulfur in GaP).

A43250